Bruno Kastler

# MRI of
# Cardiovascular
# Malformations

# MRI of Cardiovascular Malformations

Bruno Kastler

# MRI of Cardiovascular Malformations

*Author*
Bruno Kastler
Professor of Radiology and Head of Radiology
Service de Radiologie A et C
Centre Hospitalier Universitaire Jean Minjoz
bd. Alexander Fleming
25000 Besançon
France
Director of Laboratoire I4S
(Health, Innovation, Intervention, Imaging, Engineering)
Université de Franche-Comté
Besançon
France
Associate Professor of Radiology
Department of Radiology
Centre Hospitalier Universitaire
Sherbrooke, Québec
Canada
kastler@ufc-chu.univ-fcomte.fr

*This book is devoted to:*

*Children with congenital heart disease (with the hope that this book may modestly contribute to a better understanding and treatment of their disease).*

*My children, Tiphaine, Adrian and Florian (who patiently acted as dummies to prepare this atlas).*

*My nephews and nieces, Amandine, Hermance and Lysandre; Benjamin, Milena, Zelia and Aurelien.*

*My wife Blandine, already 35 years by my side.*

*Professor Wackenheim, who inspired me to illustrate pathological cases by diagrams.*

# Preface

For many years, the diagnosis of congenital cardiovascular anomalies was based on conventional radiography, catheterization and angiography. Non-invasive cardiac imaging was dramatically improved in the middle of the 1970s with the development of echocardiography, which considerably reduced the need for cardiac catheterization. This book summarizes years of "clinical collaborative work" to confirm the value of MRI, alongside echocardiography, in the management and follow-up of patients with congenital cardiovascular anomalies. This adventure began in 1987 in Strasbourg in close collaboration with Angelo Livolsi (hospital paediatric cardiologist), during examinations performed on Saturday afternoons and Sundays and often as an emergency at night, Philippe Germain (cardiologist) and Lionel Donato (hospital paediatrician). When I was appointed Professor of radiology at Besançon hospital, this adventure continued with the help of Yvette Bernard (Professor of cardiology) and her skills and competence in paediatric cardiac echocardiography.

MRI is a unique non-invasive imaging modality, a highly desirable feature in a paediatric population, which combines in one examination depicting complex cardiac anatomy measuring cardiac function and flow in one examination. The indications for MRI have been clearly established; it is perfectly complementary to echocardiography and has replaced diagnostic angiography. The primary indications are visualization of great vessels, especially coarctation of the aortic and aortic arch anomalies, right ventricular outflow tract anomalies, particularly to study the pulmonary artery and its branches, and anomalous systemic and pulmonary venous connections. MRI is also very useful for the diagnosis of complex forms and for postoperative follow-up after specific surgical procedures. Cardiac catheterization is now reserved for some types of congenital heart disease when obtaining hemodynamic information is mandatory.

The future of MRI is clearly ensured, as the spectacular progress in magnetic resonance have been accomplished these last years (imaging speed, flow analysis, angiography), will only reinforce contribution of this fundamental imaging modality and keep its indications essential.

Besancon, France                                                                                   Bruno Kastler

# Acknowledgement

I would like to thank:

Daniel Vetter for the excellent work of transcription of my diagrams in Illustrator® for Mac®.

Michel Gaudron who worked on the digital images.

Monique Dubois, Marie-Christine for updating the references.

# Contents

# Contributors

**Sebastien Aubry**  Radiologie A & C, Centre Hospitalier Universitaire Jean-Minjoz, Boulevard Fleming, 25030 Besançon, France

**Yvette Bernard**  Service de cardiologie, Centre Hospitalier Universitaire Jean-Minjoz, Boulevard Fleming, 25030 Besançon, France

**Lionel Donato**  Service de pédiatrie, Hôpital de Hautepierre, Avenue Molière, 67098 Strasbourg, France

**Philippe Germain**  Hospitaux Universitaires de Strasbourg, 1, rue de la 1re-Armée, 67000 Strasbourg, France

**George Hadjidekov**  Radiologie A & C, Centre Hospitalier Universitaire Jean-Minjoz, Boulevard Fleming, 25030 Besançon, France

**Jérome Jehl**  Radiologie A & C, Centre Hospitalier Universitaire Jean-Minjoz, Boulevard Fleming, 25030 Besançon, France

**Bruno Kastler**  Professor of Radiology and Head of Radiology, Service de Radiologie A et C, Centre Hospitalier Universitaire Jean-Minjoz, bd. Alexander Fleming, 25000 Besançon, France
Director of Laboratoire I4S (Health, Innovation, Intervention, Imaging, Engineering), Université de Franche-Comté, Besançon, France
Associate Professor of Radiology, Department of Radiology, Centre Hospitalier Universitaire, Sherbrooke, Québec, Canada

**Laurent Laborie**  Radiologie A & C, Centre Hospitalier Universitaire Jean-Minjoz, Avenue Molière, 67098 Strasbourg, France

**Angelo Livolsi**  Service de pédiatrie, Hospitaux Universitaires de Strasbourg, Hôpital de Hautepierre, Avenue Molière, 67098 Strasbourg, France

**Philippe Manzoni**  Radiologie A & C, Centre Hospitalier Universitaire Jean-Minjoz, Boulevard Fleming, 25030 Besançon, France

**Armand Parsai**  Radiologie A & C, Centre Hospitalier Universitaire Jean-Minjoz, Boulevard Fleming, 25030 Besançon, France

**Daniel Vetter**  Service IRM, Hospitaux Universitaires de Strasbourg, Hôpital de Hautepierre, Avenue Molière, 67098 Strasbourg, France

# Patient Preparation: Magnetic Resonance Imaging Techniques

Magnetic resonance imaging plays a major role in the assessment of congenital heart disease [1–3]. The general principles of image acquisition are the same as in other clinical settings, but the assessment of congenital heart disease presents a number of specific features, which are described in this chapter by reviewing the main sequences used and their clinical value.

## 1.1 Examination Conditions

As in adults, cardiovascular MRI does not constitute an emergency examination for two essential reasons: the difficulties of patient surveillance during the examination and, especially, the very limited availability of MR machines that are already severely overbooked.

As an elective procedure, the major difficulty consists of ensuring good patient immobilization during the examination. Three main situations can be distinguished according to the child's age:

- In very young patients (especially below the age of 3–6 months), good immobilization is generally obtained quite easily during sleep following a feed.
- Similarly, when the examination can be explained to the child and when the parents are allowed to stay beside the MR apparatus, this examination can generally be performed in children older than 6 or 7 years without any particular medication for fairly short examination times.
- In contrast, the situation is much more difficult in children between the ages of 1 and 6 years. If sufficient time is available (at the end of the day's programme), MRI can be performed without anaesthesia, by lightly sedating the child with chloral hydrate solution administered after the baby's bottle or with intrarectal Hypnovel® (midazolam). This generally ensures satisfactory immobilization within about 30 min, and repeated sequences can be launched during this interval. When this waiting time is not available, MRI must be performed in coordination with an anaesthetist. Some radiologists immobilize the child with Velpeau® bandages in plastic frames designed to be installed inside the coil.

In extreme cases, when anaesthesia must be avoided, good results can be obtained by letting an agitated child fall asleep on its mother's stomach (Fig. 1.1).



**Fig. 1.1** A 4-year-old child, refractory to the usual sedatives, lying on his mother's stomach. Gating with the child's ECG allowed satisfactory imaging of the left ventricular walls (see Fig. 1.11). This last resort method can be effective when anaesthesia must be avoided, but the use of a whole body coil leads to a marked reduction of the signal-to-noise ratio for the analysis of small anatomical structures

A coil with a good apparent diffusion coefficient must be used, preferably a quadrature coil. A "head" coil or "knee" coil is generally used in young patients and a "chest" coil is used in older children. The region to be studied must be positioned in the centre of the coil. The child must be comfortably placed and well covered, and ventilation in the tunnel may need to be turned off. Baby vests must not have any metal clips or safety pins.

Small ECG electrodes with carbon contact clips and no metal parts must be arranged to obtain a good amplitude ECG recording with a clearly visible monophasic R wave to ensure reliable gating.

## 1.2  Sequences Used

The major difference in relation to adult imaging concerns the naturally high heart rate of infants (110–150 bpm). Gating of sequences with the R wave of the ECG therefore provides only a brief time window for signal acquisition, making it impossible to obtain 10–12 slices (on multislice spin-echo sequences) or 20–30 cardiac cycles (by cine-MRI) as in adults, but only about one quarter of these imaging rates. On the other hand, sequences are more rapidly completed in view of the rapid heart rate when cardiac gating is satisfactory (gating for each heart beat and not for every two or three heart beats). Only T1 weighting is possible due to the short TR related to the rapid heart rate (i.e. morphological imaging, without clearly defined tissue characterization). It should be noted that, in ECG-gated multislice imaging, each image is obtained at a distinct instant of the cardiac cycle, as shown in Fig. 1.2.

A 200-mm field of view with a 160 (anteroposterior) × 256 matrix is usually used to acquire images with a slice thickness of 3–5 mm and 2–4 accumulations, which corresponds to a resolution in the imaging plane of about 1 mm with an acquisition time of about 4 min. On modern machines, equipped with powerful gradients (fast imaging), the noise generated by gradient switching constitutes a considerable problem, as this noise can sometimes be very strident and intense and can wake or frighten the sleeping child, in which case, some sequences may need to be avoided (a "*quiet*" mode is available on some machines).

Four types of sequences are distinguished according to the desired type of information (Table 1.1).

Ultrafast or real-time imaging (for example, echo-planar imaging which produces an image in 100 ms)
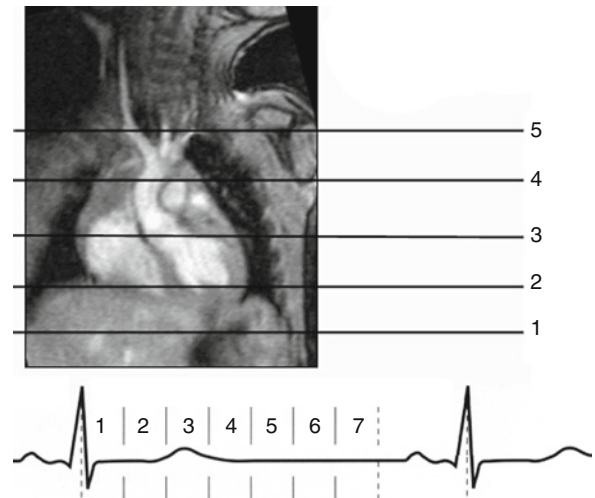


**Fig. 1.2** In ECG-gated multislice imaging, each slice corresponds to a distinct instant of the cardiac cycle. Some images are therefore acquired in diastole, while others are acquired in systole; this acquisition mode is consequently unsuitable for precise measurements, which must be performed on cine images, on which diastole and systole are well defined

**Table 1.1**  Four types of sequences are used

| Approach | Type of sequence | Application |
|---|---|---|
| Morphological | Black-blood: spin-echo and variants, double IR prepared | Anatomy of structures |
| Kinetic | Bright-blood: gradient-echo cine-MRI, balanced-SSFP | Wall motion and blood flow |
| Flowmetric | Velocity mapping | Flow quantification (especially shunts) |
| Angiographic | With or without gadolinium | Vascular imaging |

does not have a satisfactory spatial resolution and contrast at the present time, but can be useful for localizing sequences.

## 1.3  Morphological Approach

The primary indication for MRI is generally morphological analysis, which is usually obtained by black blood techniques (low signal of flowing blood) and is based on spin-echo techniques.

Spin-echo-based sequences provide fairly good natural contrast between cardiac chambers (and/or
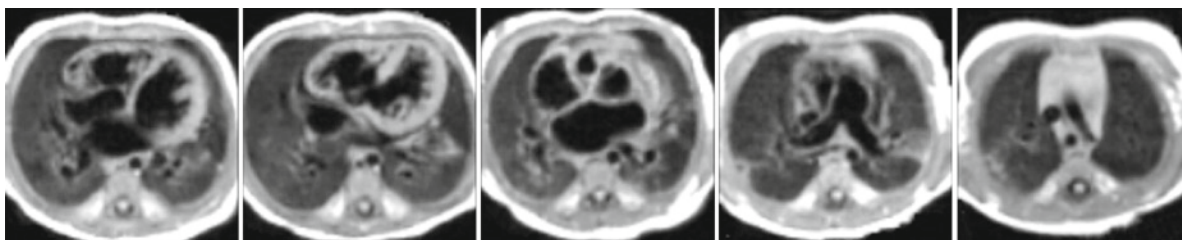
**Fig. 1.3** Axial spin-echo sequence in a neonate with transposition of the great vessels. Several successive acquisitions were performed (0.5 T) (see Chaps. 3 and 7)

vessels lumen), in which mobile spins present a low signal intensity, in contrast to the walls, which present a higher signal intensity.

MR imaging sequence, including spin-echo-based techniques, has benefited from constant technical progress with the primary emphasis on speed.

It must, however, be outlined that bright-blood techniques (enhanced signal of inflow blood), particularly, the recently introduced balanced-SSFP, generate fast images with high spatial resolution, which offer highly detailed anatomical information.

### 1.3.1 Conventional Spin-Echo Sequence

Classically, the multislice spin-echo sequence is used with 2–4 imaging planes according to the child's heart rate. Several serial contiguous acquisitions can be used to acquire a larger volume (Fig. 1.3).

The spatial resolution of these T1-weighted images (short TR dictated by the rapid heart rate in infants) is satisfactory (about 1 mm in the plane of view). The acquisition time can be shortened by adopting asymmetrical matrices adjusted to the structures studied [4]. Several accumulations are necessary for thin slices (3 mm). A disadvantage of this sequence, that can sometimes be prohibitive, concerns the artefacts propagated in the direction of phase coding, which can become very important at high fields (Fig. 1.4). As these artefacts are essentially related to respiratory movements, swapping the direction of phase and frequency encoding can reduce them.

### 1.3.2 Variants

Variants of the spin-echo sequence have been proposed aiming at increasing imaging speed and optimizing image quality.



**Fig. 1.4** Artefacts (classical spin-echo) obtained along the phase-encoding direction (in this case anteroposterior) related to respiratory (*long arrow*) and cardiac (*large arrow*) movements in a case of poor cardiac gating

### 1.3.3 Fast Spin-Echo or Turbo-Spin-Echo

On these sequences, 2–12 phase coding steps are obtained after each excitation (segmented imaging). The acquisition time is consequently divided by the corresponding turbo factor. The main purpose of these sequences is to provide identical spatial resolution to that of classical spin-echo sequences with a shorter acquisition time. Potential limitations of fast spin-echo sequences include blurring due to signal variation from

one line of k space to the other and respiratory motion artefacts. Respiratory motion algorithm or navigator echo techniques using diaphragmatic motion have been proposed. Fast spin-echo acquisition time is compatible with breath-holding, which is essential to prevent motion artefacts. These sequences provide the best image quality when breath-holding (possible in elderly cooperative children or adults) is performed correctly. However in our experience, this type of sequence has proven useful in paediatric cardiology, despite respiratory movements.

### 1.3.4 Double IR Sequences

Another drawback of fast spin-echo sequences is incomplete blood signal, stagnant blood being mistaken as tissue. A double inversion pulse has been added at the beginning of the sequence for blood signal suppression and optimization of black blood imaging [5, 6]. First a non-selective 180° pulse occurs at the r wave trigger. A second selective 180° pulse restores the signal of section to be imaged (cardiac walls higher signal), whereas the nulled blood (black signal) flows in at a specific inversion time (TI). Single slice or better multislice double IR T2-weighted black blood sequences allowing excellent image quality during one breath-hold [7] are now becoming gold standard for black blood imaging and used routinely in replacement of fast spin-echo sequences. Double IR sequences can be combined with half Fourier acquisition.

### 1.3.5 Half Fourier Single Shot Fast Spin-Echo Sequences

An extreme version of Fast spin-echo imaging consists of completing, in a single passage, a half Fourier acquisition by means of echo signals generated by many refocusing RF impulses (typically 80) following the initial excitation at 90° (HASTE-Siemens, SSFSE-GEMS, SSTSE-Philips). These T2-weighted sequences present a major advantage in terms of speed, images being acquired within a heartbeat [8, 9], but the spatial resolution remains fairly poor and the use of a half Fourier acquisition makes the sequence very sensitive to spectral folding and motion artefacts (Fig. 1.5).

**Fig. 1.5** Example of the results obtained with a Haste sequence (very rapid variant of spin-echo sequence), requiring only one heart beat. Spatial resolution is limited and several artefacts related to the use of a half Fourier acquisition are observed, but this type of sequence is very useful in practice due to its very short acquisition time, when breath-hold images cannot be obtained in young children

When available, half Fourier single shot FSE sequences, because they are very rapid, provide useful sets of localizing images and are a valuable alternative in patients unable to hold their breath. This type of sequence delivers a large number of 180° radiofrequency pulses, and can cause RF energy deposit and patient overheating (see: febrile patient), which is why limitation devices, taking the patient's weight into account, must be used (SAR). Black blood sequences should be performed before gadolinium injection as this latter impairs proper blood suppression by the specific unselective IR pulse.

## 1.4 Gradient-Echo Cine Imaging

Gradient-echo techniques offer two advantages for cardiovascular imaging: good visualization of the hyperintense blood pool, and cine imaging, which is very useful to assess contraction of the cardiac walls and blood flow.

The contrasts obtained on gradient-echo sequences are practically inverted compared to spin-echo sequences, as illustrated in Fig. 1.6. The dark colour of circulating blood, visible on spin-echo, is replaced by a

**Fig. 1.6** (**a**) Spin-echo sequence (blood is black, walls have an intermediate signal intensity). (**b**) Gradient-echo sequence (blood is white, walls have an intermediate signal intensity)

gradient (Flash-Siemens, FFE-T1 Philips, SPGR-GE) and others restore transverse magnetization by steady-state (FISP-Siemens, FFE-T2 Philips, Grass-GE). The most useful techniques recently introduced in cardio-vascular imaging now use balanced and symmetrical flow compensating gradients: Balanced-SSFP (Fiesta/GE, True-FISP/Siemens, Balanced-FFE/Philips). These sequences generate cine-MRI (with T2/T1 image weighting) [10] and furthermore excellent anatomical details. Advantages include faster imaging, better blood pool signal enhancement not relying on inflow effects and higher SNR. Drawbacks are sensitivity to field inhomogeneity (metallic artefacts, magnetic susceptibility), motion artefacts (respiration, pulsatile through plane flow under certain conditions), and most of all, significantly less sensitivity to abnormal flow patterns (flow void jets due to stenosis, regurgitation, ASD, VSD) in comparison to traditional GE cine-MRI. In view of the above-mentioned limitations, traditional GE cine-MRI is still performed. Unlike black blood techniques, it can be performed not only before but also after gadolinium administration.

### 1.4.1 Beating Heart Applications

The succession of diastolic and systolic images during the cardiac cycle allows assessment (and possibly quantification) of global and segmental wall contraction [11]. This application is less useful in children than in adults, but may be useful for assessment of cardiomyopathies (especially right ventricular dysplasia) or ischaemic disease (Fig. 1.10).

### 1.4.2 Qualitative Assessment of Blood Flow Applications

Another advantage of gradient-echo sequences concerns signal void, which occurs in the blood pool in the case of very rapid or turbulent flow (stenoses or regurgitating valves, flow jets in shunts), which cause flow void jets across the hyperintense blood pool corresponding to disturbances of flow [12, 13]. However, this pathological sign remains purely qualitative and not quantitative, as the dephasing effects are related to the TE time (the longer the TE, the more intense is the

high signal intensity of the blood pool on gradient-echo images. Muscle (and myocardial) tissue presents an intermediate signal intensity (grey) and adipose tissue has a high signal intensity on both types of sequences. The two examples shown in Figs. 1.7 and 1.8 illustrate the differences between spin-echo and gradient-echo sequences. One of the advantages of these differential contrasts is to facilitate identification of air and vascular structures, as shown in Figs. 1.8 and 1.9.

Gradient-echo therefore constitutes a useful complement to spin-echo for multislice anatomical imaging, but most importantly, these sequences allow repeated acquisition in the same plane at different successive instants of the cardiac cycle. Closed loop visualization of these images corresponds to the cine mode, which is very useful for cardiac applications. There are several types of gradient-echo sequences: some dephase transverse magnetization with a dephasing

**Fig. 1.7** Example of anomalous pulmonary venous connection of the right inferior pulmonary into the inferior vena cava (*arrow*); this child also presents azygos continuation of the inferior vena cava (see Chap. 4, Fig. 19). (**a**) Spin-echo sequence. (**b**) Gradient-echo sequence (cine-MRI). Tracheobronchial structures have low signal intensity on both sequences, while vessels have low signal intensity on spin-echo sequences and high signal intensity on gradient-echo sequences
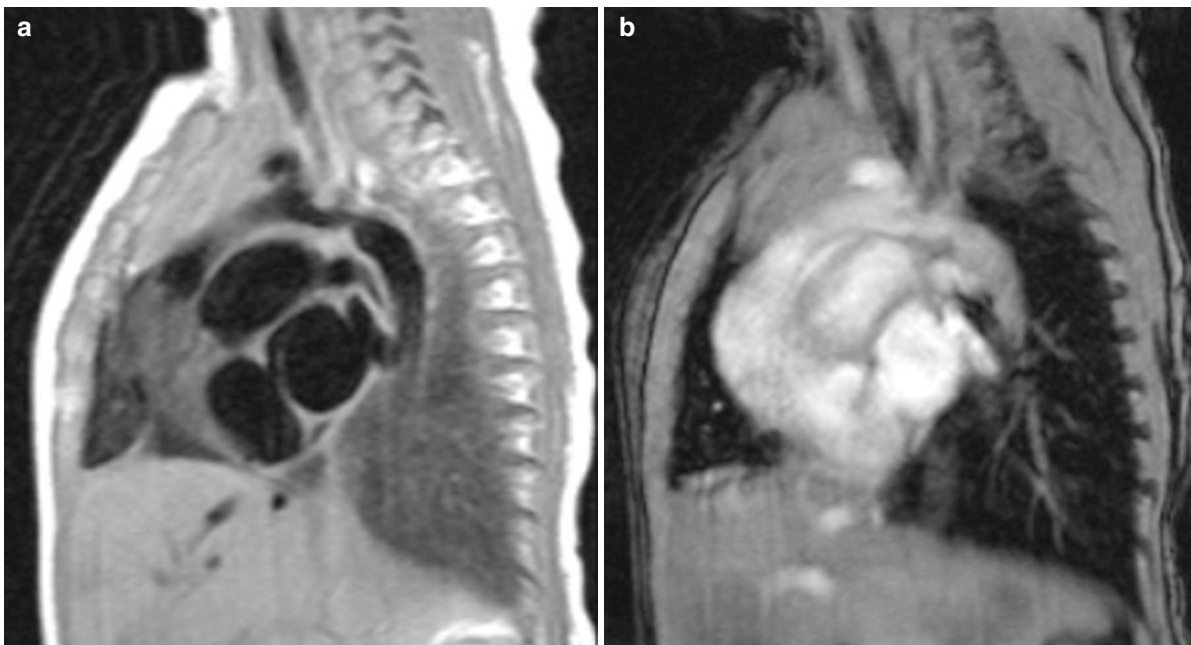


**Fig. 1.8** Sagittal oblique images in an infant with D-transposition of the great vessels. (**a**) Spin-echo sequence. (**b**) Gradient-echo sequence. Pathognomonic "gun barrel" appearance of the aorta (anterior) and pulmonary artery (dilated, posterior). Inversion of vascular contrast between the two sequences

**Fig. 1.9** Aortic arch anomaly (Neuhauser anomaly, see Chap. 5, Fig. 13) on two different axial slices. The advantage of gradient-echo (cine images on the *right*) compared to spin-echo (images on the *left*) is that it clearly demonstrates vascular structures
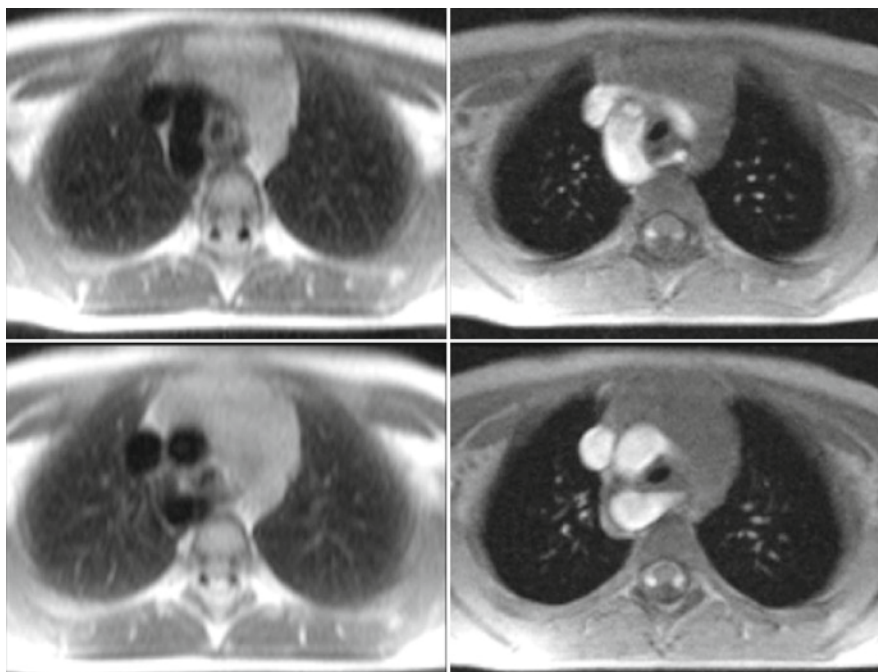


signal void). In practice, it is a very useful sign (as in colour-coded duplex echocardiography), for example, to estimate the extent of valvular regurgitation (Fig. 1.11) or to detect a left–right shunt (Fig. 1.12). As mentioned earlier, balanced-SSFP sequences are now used routinely in place of traditional GE cine-MRI. However, when abnormal flow pattern analysis is required, traditional GE cine-MR (with optimized long TE) should still be performed.

## 1.5 Phase Velocity Mapping for Flow Quantification

Phase velocity mapping sequences [14, 15] are based on phase encoding of the NMR signal proportionally to the velocity of spins in a given direction (generally perpendicular to the imaging plane). Phase velocity mapping sequences are gradient-echo cine sequences with slightly modified gradients.

The flow velocity curve during the cardiac cycle can be extracted from the phase images obtained for various arterial or venous regions of interest. Figure 1.13 illustrates the use of this sequence to measure aortic blood flow. The blood flow rate $Q$ in this region during each cardiac cycle can be easily determined from the mean flow rate $V$ and the surface area of the region of interest $S$: $Q_{mL/cycle} = V \times S$. It should be noted that, as for duplex echocardiography, velocity is more severely underestimated as the direction of flow shifts from the plane perpendicular to the imaging plane. This technique can therefore be used only when the imaging plane is perpendicular to the vessel studied. Finally, the range of velocities to be encoded must be carefully selected to avoid aliasing phenomena when the flow velocity exceeds the encoding range (as in Doppler). Prior definition of the direction of flow and its order of magnitude is therefore essential to obtain good measuring conditions.

### 1.5.1 Measurement of the QP/QS Shunt Ratio

The main application of this technique in congenital heart disease is non-invasive measurement of shunt ratios [16, 17] by comparison with pulmonary (QP, typically measured in the pulmonary artery trunk) and systemic blood flow (QS, typically measured in the ascending aorta). Figure 1.14 illustrates this concept in a case of ostium secundum ASD. Two separate acquisitions must be performed in this case due to the

**Fig. 1.10** Diastolic and systolic images from cine-MRI sequences obtained in the child presented in Fig. 1.1. This 4-year-old boy suffered from Kawasaki disease inducing anterior myocardial infarction. An attempt to visualize the coronary arteries failed, but cine imaging clearly shows the large anterior akinetic area (*arrows*). The ejection fraction can be calculated by planimetry of the diastolic and systolic ventricular contours
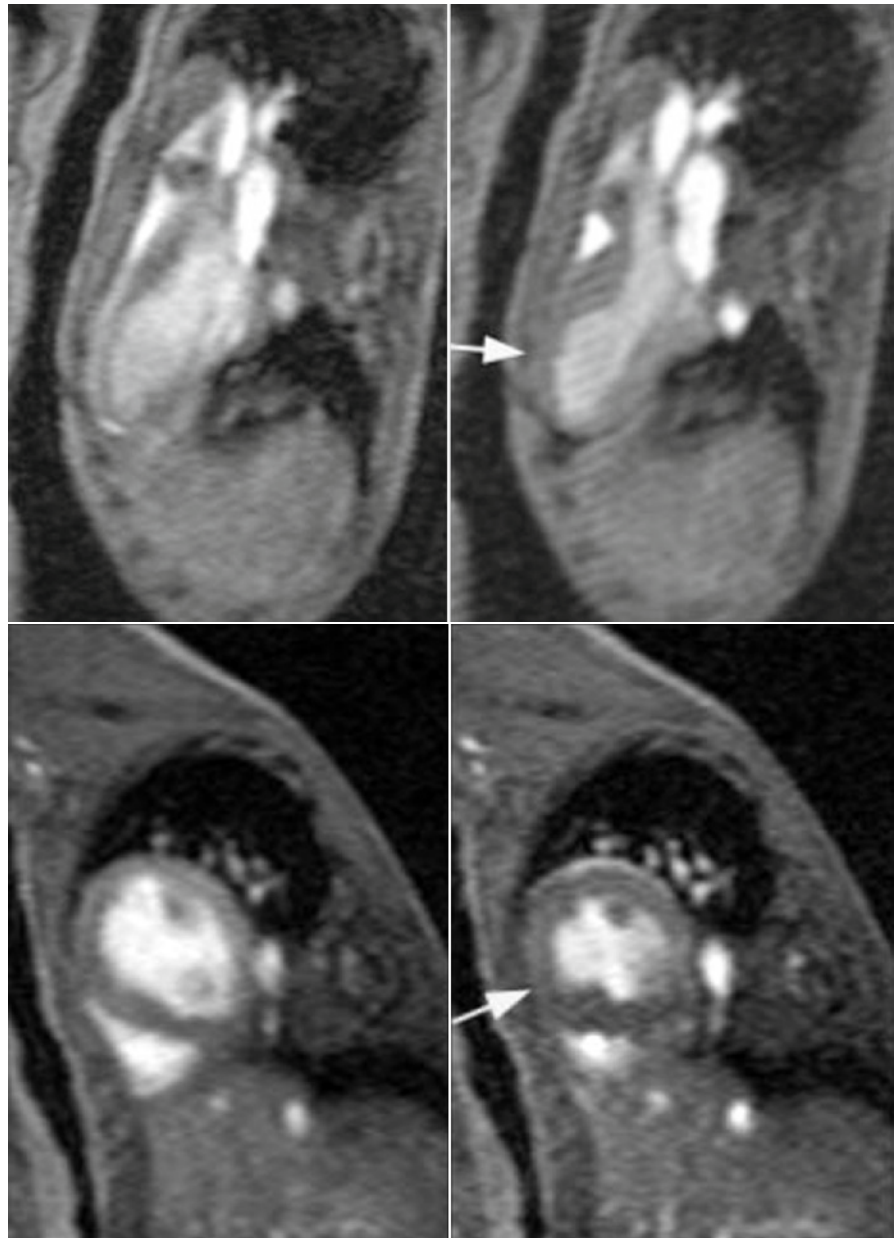


different orientations of the ascending aorta (vertical) and pulmonary artery trunk (inclined superiorly and posteriorly). Velocity measurements are usually corrected by a complementary measurement performed on a static region (muscle tissue) to correct for any systematic dephasing. As the flow rate measured is proportional to the surface area of the region of interest, vascular margins must be very carefully contoured, as the acceptable error is ± 10%.

## 1.5.2 Assessment of Direction of Flow

When velocity encoding gradients are applied in the imaging plane (and not perpendicular to this plane), phase images indicate the direction of flow in the imaging plane. One of the possible applications is analysis of the false channel in aortic dissection, to determine whether or not it is circulating (complication of Marfan syndrome, for example). Assessment
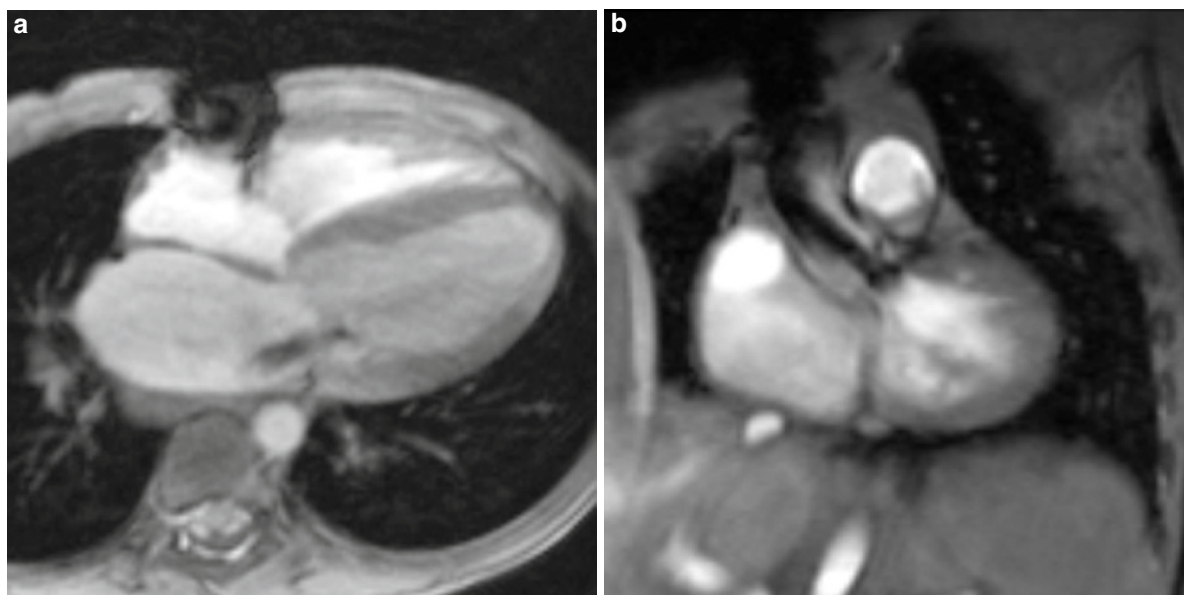
**Fig. 1.11** Systolic gradient-echo cine images obtained in an infant with mitral regurgitation (**a**) and congenital aortic stenosis (**b**). Trails of signal void indicate the presence of rapid and turbulent jets related to valvular lesions

of flow lines is also useful to define the region with the highest velocity, to select the zone in which flow quantification can be used to calculate pressure gradients (Figs. 1.15 and 1.16).

### 1.5.3 Pressure Gradient Estimation

Like Doppler echocardiography, MRI can be used to estimate pressure gradients $\Delta P$ across stenotic segments, from the maximum velocity $V$, according to the simplified Bernouilli equation $\Delta P = 4 \times V^2$. An important application concerns coarctation of the aorta [18, 19]. An example of pressure gradient measurement in pulmonary stenosis is shown in Fig. 1.16. However, certain difficulties of this approach must be emphasized.

- Echo times (TE) must be very short to avoid intravoxel dephasing which would induce signal loss and therefore loss of information at the site of measurement.
- To avoid underestimating the gradient, the measurement must be performed precisely at the site of maximum stenosis. For these reasons, pressure gradient measurement is difficult to perform in practice.

These velocity mapping sequences therefore constitute a very useful complement to conventional anatomical imaging, as they provide a supplementary, functional dimension, particularly for comparative right–left flow quantification or to estimate flow in Blalock-Taussig shunts, for example.

### 1.5.4 MR Angiography

Gradient-echo sequences already provide a good "angiographic" approach, as shown in Figs. 1.7–1.9. MR angiography differs from standard sequences by a technique designed to achieve maximum contrast between stationary tissues and circulating blood, and also by projective rather than tomographic presentation of the data. The operation of transformation of raw data (stacks of parallel images) into projections oriented in any direction is called MIP (maximum intensity projection). Three main principles of MR angiography are currently used. The first two do not require injection of contrast agent [20–23] and are based on phase modulation of the spins or the time of flight (TOF) effect. The third method is the most effective and is based on enhancement of the intravascular signal following bolus injection of gadolinium (contrast-enhanced angiography) [22–25].
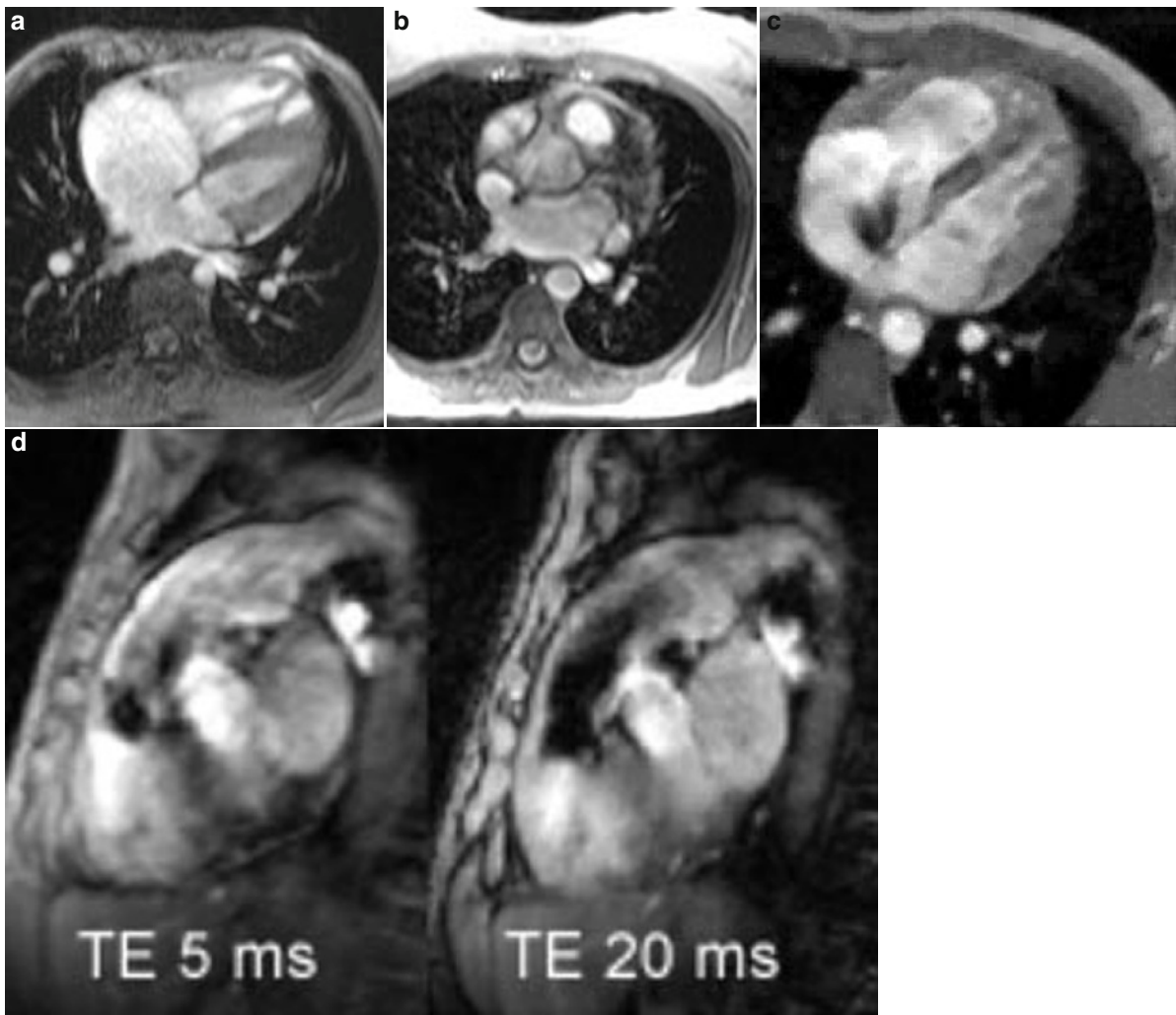
**Fig. 1.12** Value of gradient-echo cine sequences for the analysis of shunts. In the presence of a large atrial septal defect, the flow velocities corresponding to the shunt can be low. In this case, there is no visible signal void, but the defect is often more clearly visualized than on spin-echo sequences (image (**a**) with large ostium secundum ASD and (**b**) high sinus venosus ASD). When flow velocities in the defect are higher ((**c**) ASD and (**d**) high VSD), the jet has a signal void appearance (*black*). Image (**d**) shows that the infundibular signal void is more marked with a long TE (20 ms) than with a short TE (5 ms). The MR signs of pathological jet must therefore be interpreted cautiously in the light of the results obtained with a sequence with which the radiologist is more familiar

## 1.5.5 Non-enhanced MR Angiography

Phase-contrast angiography is well adapted to the study of slow flows, but is not suitable for infants or children, who present fairly high and very pulsatile circulatory velocities. The TOF technique is more appropriate for these situations, but blood flow must be perpendicular to the imaging plane. The entry of fully magnetized, unsaturated spins into the imaged slice, in contrast with the already saturated spins of the surrounding tissues,

**Fig. 1.13** Flow measurement in the ascending aorta during the cardiac cycle. The image is acquired perpendicular to the ascending aorta. The phase image corresponds to the velocity mapping perpendicular to the imaging plane (systolic image). The graph on the *right* shows the mean velocity measured at each instant of the cardiac cycle in the region of interest corresponding to the ascending aorta. The integral of the velocities in this zone of interest corresponds to aortic systolic flow (ejection flow)
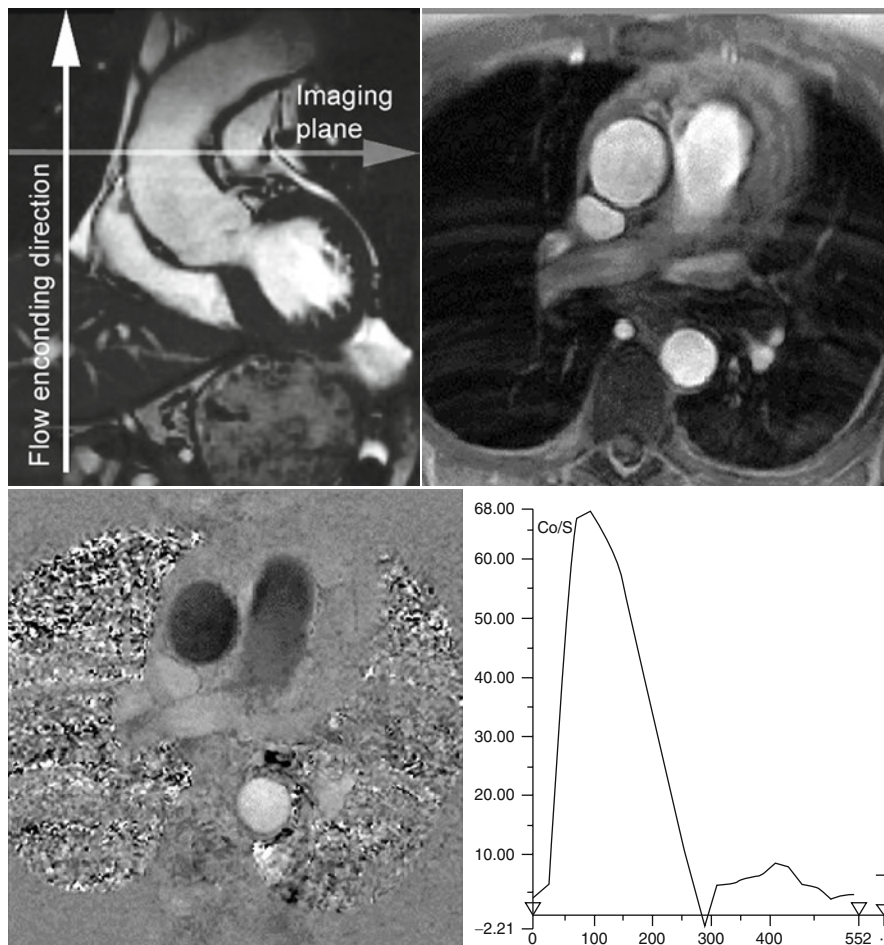


induces excellent vascular contrast. In addition, saturation pulses can be applied above or below the imaged slice to selectively suppress venous or arterial flow, as shown in Fig. 1.17.

TOF sequences can be acquired in 2DFT (successive acquisitions of thin separate images) or 3DFT (global acquisition of a volume composed of elementary partitions) modes. The 2DFT mode provides optimal vascular contrast, but a poor signal-to-noise ratio. In 3DFT mode, the signal-to-noise ratio is better, but saturation effects are observed as blood travels in the imaged volume, which decreases vascular contrast. Forty to sixty 2 mm thick images are usually acquired in about 6–8 min.

### 1.5.6 Contrast-Enhanced MR Angiography

The best results at the present time are obtained with fast 3DFT sequences, acquired during first passage of a T1 contrast agent. These gradient-echo sequences (TR about 5 ms and TE about 2 ms) allow about thirty 1–2 mm thick images to be obtained in about 10 s for a limited resolution (1.5 mm pixels, for example) and about 20 s for a higher resolution (pixels measuring about 1 mm) (Fig. 1.18).

Apart from rapid acquisition, compatible with one breath-hold in older children and adults, the decisive advantages are:

**QP/QS shunt ratio measurement
in a patient with ASD**

Slice perpendicular to the aortic root

**Modulus image**     **Phase image**

Slice perpendicular to the pulmonary artery

QP/QS = 220/66 = 3,3

QS : 66 ml/systole

QP : 220 ml/systole
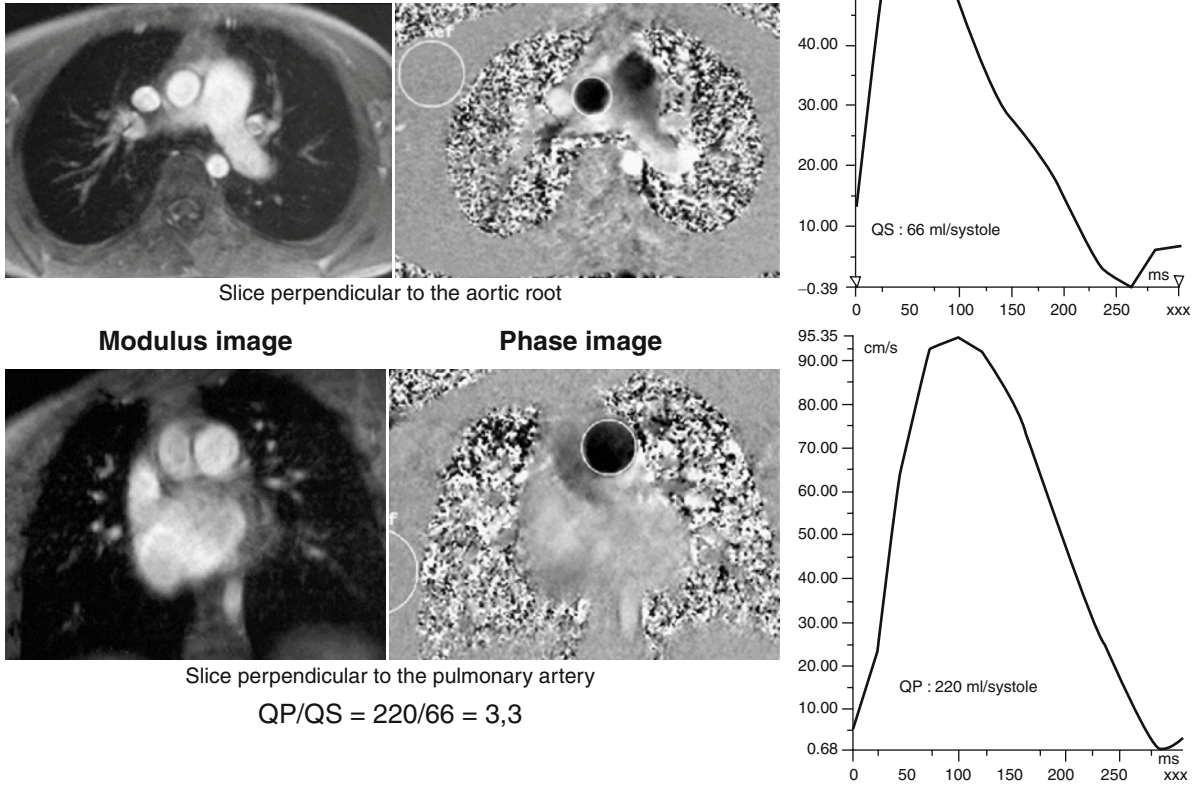
**Fig. 1.14** Example of measurement of a shunt ratio in a 6-year-old boy with ostium secundum ASD. On the *top part* of the figure, the measurement is performed perpendicularly to the ascending aorta. The "modulus" image is on the *left* and the corresponding "phase" image (systole) is in the *middle*. Velocity curves in the cardiac cycle are shown on the *right*. The *bottom* images show measurement in another imaging plane, perpendicular to the pulmonary artery trunk. In this case, the shunt ratio is high (QP/QS = 220/66 = 3.3). This measuring modality is relatively easy and appears to be reliable
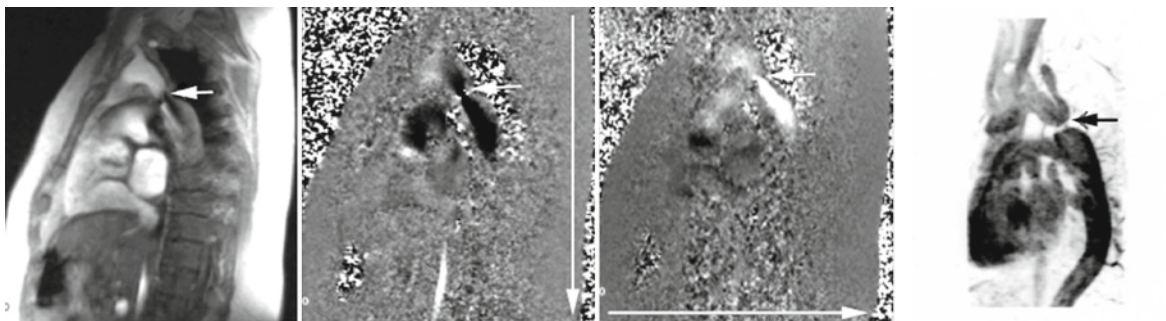


**Fig. 1.15** Sagittal oblique images obtained in a young girl with coarctation of the aorta. The image on the *left* corresponds to a systolic gradient-echo "module" image through the isthmic coarctation (*arrow*). The *middle* images correspond to velocity mapping images obtained after velocity coding in the imaging plane in the craniocaudal (*vertical long arrow*) and anteroposterior (*horizontal long arrow*) directions. The highest velocities are observed in the zone of maximum strangulation of the coarctation. The image on the *right* corresponds to gadolinium-enhanced MR angiography (Dota-Gd, Guerbet, France)
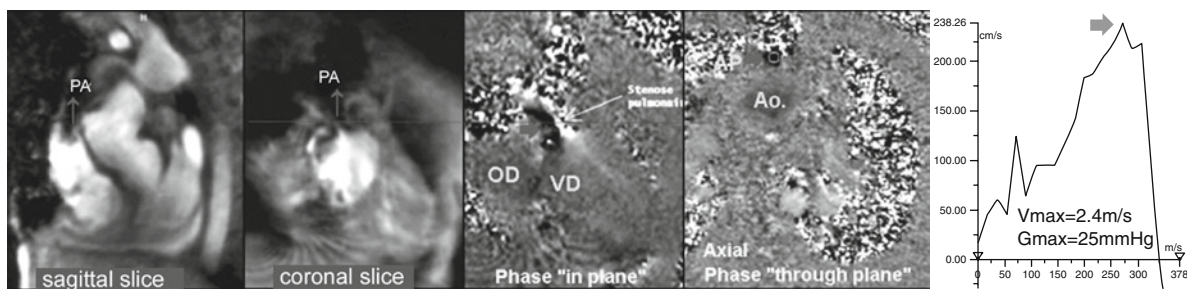
**Fig. 1.16** Example of pulmonary valve stenosis. The two images on the *left* correspond to systolic "module" images obtained in the coronal and sagittal planes. The *middle* image is a coronal image showing the axial plane used to measure veloci-ties. The maximum velocity measured in the pulmonary artery (*arrows*) was 2.4 m/s, which corresponds to a pulmonary gradi-ent of about 25 mmHg
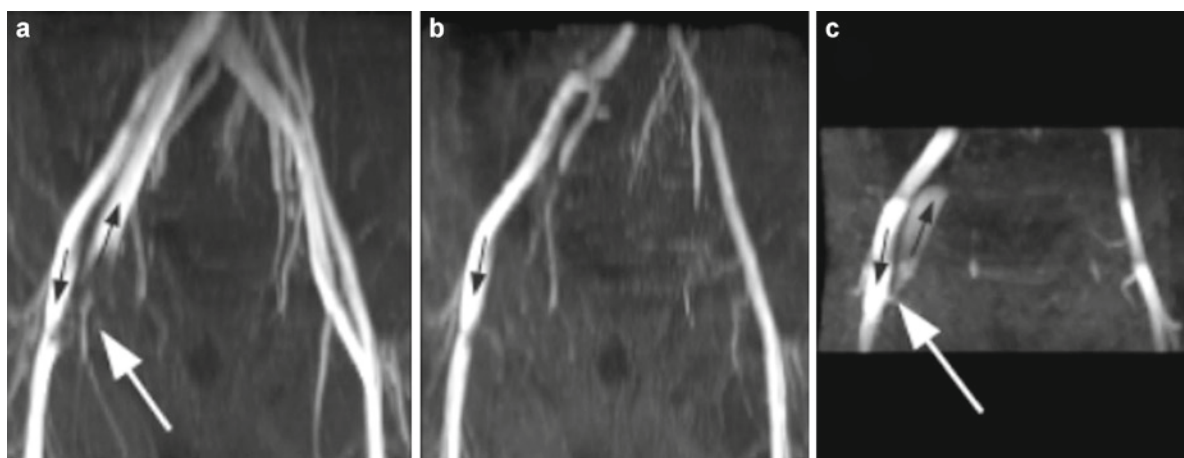


**Fig. 1.17** TOF MR angiography (without injection of contrast agent) obtained in a 12-month-old infant with right femoral arte-riovenous fistula. (**a**, **b**) Correspond to 2DFT acquisitions (stacks of serial thin axial slices). No presaturation is applied in image (**a**). The venous signal void over the fistula is related to turbu-lence in the shunt (*white arrow*). More distally, the right iliac vein is dilated compared to the contralateral vein. In (**b**), venous presaturation (inferior) is applied to each slab suppressing all venous signals (including distal to the fistula), leaving only the arteriogram. The image on the *right* (**c**) corresponds to a 3DFT acquisition in three slabs with underlying venous presaturation of each slab. A venous signal related to the shunt is visible in the central image

- Large field of view with no constraints related to the direction of flow compared to the imaging plane as in the case of the TOF technique.
- Excellent vascular contrast due to the marked reduc-tion of T1 induced by passage of gadolinium bolus.
- 3D MIP reconstruction and time-resolved dynamic sequences [26] allowing evaluation of small vacular structure patency and separation of the venous and arterial phases and of pulmonary and systemic cir-culation (see Fig. 1.14 E, F Chap. 7).

However, this technique presents certain limitations. A good quality venous line must be set up to allow a suf-ficient bolus injection rate. The choice of imaging vol-ume is critical, as it must be sufficiently large to include all of the vascular structures of interest, but must be sufficiently small to allow an acceptable acquisition time. Finally, the interval between injection and launching of the sequence must be precisely adjusted so that the time of acquisition of the central line of the Fourier plan (start or middle of the sequence) exactly corresponds to the time of passage of the gadolinium
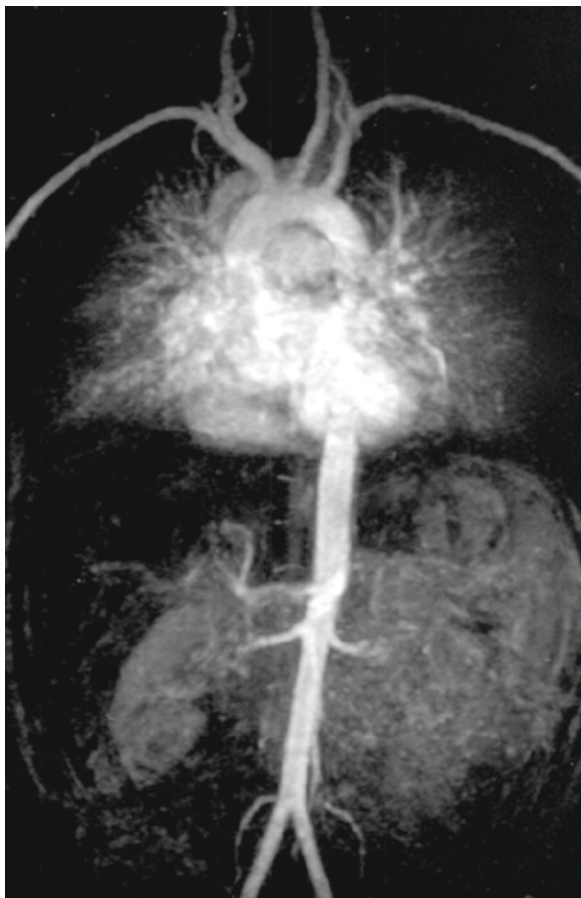
**Fig. 1.18** MR angiography obtained in 8 s in a 6-year-old boy with injection of 4 mL of gadolinium (0.2 mL/kg). A large field of view can be obtained in this small child with an adult chest coil extending from the origin of supra-aortic vessels to the iliac vessels



**Fig. 1.19** Examples of abdominal coarctation of the aorta in an adolescent, visualized by gadolinium-enhanced MR angiography (Dota-Gd, Guerbet, France), with a brief breath-hold of 10–20 s (see Chap. 6). MIP projections comprise bothersome superimposition effects, poor distinction between the stenotic abdominal aorta and the origin of the coeliac trunk, which is why, analysis of elementary images or multiplanar reconstructions in other planes is essential to ensure correct interpretation of the examination

bolus. This factor makes MR angiography of the right ventricular outflow tract and pulmonary branches particularly difficult due to the very rapid transit in these structures. Figure 1.19 provide several examples of the results obtained with this technique which, in the future, should considerably limit the indications for conventional angiography (except for coronary vessels).

## 1.6    Conclusion

Multiple sequences can be used in paediatric cardio-vascular MRI. The examination must not be limited to purely morphological imaging, but must also take

advantage of the possibilities of functional imaging provided by cine-MRI techniques, velocity mapping and MR angiography.

## References

1. Higgins CB, editor. MRI of congenital heart disease. In: Essentials of cardiac radiology and imaging. New York: J.B. Lippincott; 1992. p. 283–331.
2. Ho VB, Kinney JB, Sahn DJ. Contributions of newer MR imaging strategies for congenital heart disease. Radiographics. 1996;16:43–60.

3. Bank ER. Magnetic resonance of congenital cardiovascular disease. An update [review]. Radiol Clin North Am. 1993;31:553–72.

4. Kastler B, Livolsi A, Germain P. Strip scanning a method to improve pediatric cardiovascular MRI. In: SMRI, Ninth Annual Meeting, Chicago; 3–6 April 1991.

5. Edelman RR, Chien D, Kim D. Fast selective black blood MR imaging. Radiology. 1991;181(3):655–60.

6. Simonetti OP, Finn JP, White RD, Laub G, Henry DA. "Black blood" T2- weighted inversion-recovery MR imaging of the heart. Radiology. 1996;199(1):49–57.

7. Boiselle PM, White CS. New techniques in cardiothoracic imaging. New York: Informa Healthcare USA; 2007. p. 81–2.

8. Stehling MK, Holzknecht NG, Laub G, Böhm D, von Smekal A, Reiser M. Single-shot T1- and T2-weighted magnetic resonance imaging of the heart with black blood: preliminary experience. MAGMA. 1996;4(3–4):231–40.

9. Winterer JT, Lehnhardt S, Schneider B, Neumann K, Allmann KH, Laubenberger J, et al. MRI of heart morphology. Comparison of nongradient echo sequences with single- and multislice acquisition. Invest Radiol. 1999;34(8): 516–22.

10. Carr JC, Simonetti O, Bundy J, Li D, Pereles S, Finn JP. Cine MR angiography of the heart with segmented true fast imaging with steady-state precession. Radiology. 2001;219(3):828–34.

11. Graham TP Jr. Ventricular performance in congenital heart disease. Circulation. 1991;84:2259–74.

12. Mohiaddin RH, Longmore DB. Functional aspects of cardiovascular nuclear magnetic resonance imaging. Techniques and application [review]. Circulation. 1993;88:264–81.

13. Weber OM, Higgins CB. MR evaluation of cardiovascular physiology in congenital heart disease: flow and function. J Cardiovasc Magn reson. 2006;8(4):607–17.

14. Rees S, Firmin D, Mohiaddîn R, Underwood R, Longmore D. Application of flow measurements by magnetic resonance velocity mapping to congenital heart disease. Am J Cardiol. 1989;64:953–6.

15. Rebergen SA, Niezen RA, Helbing WA, van der Wall EE, de Roos A. Cine gradient-echo MR imaging and MR velocity mapping in the evaluation of congenital heart disease. Radiographics. 1996;16(3):467–81.

16. Brenner LD, Caputo GR, Mostbeck G, et al. Quantification of left to right atrial shunts with velocity-encoded cine nuclear magnetic resonance imaging. J Am Coll Cardiol. 1992;20:1246–50.

17. Boehrer JD, Lange RA, Willard JE, Grayburn PA, Hillis LD. Advantages and limitations of methods to detect, localize, and quantitate intracardiac left- to-right shunting [review]. Am Heart J. 1992;124:448–55.

18. Oshinski JN, Parks WJ, Markou CP, et al. Improved measurements of pressure gradients in aortic coarctation by magnetic resonance imaging. J Am Col Cardiol. 1996;28: 1818–26.

19. Simpson IA, Chung KJ, Glass RF, Sahn DJ, Sherman FS, Hesselink J. Cine magnetic resonance imaging for evaluation of anatomy and flow relations in infants and children with coarctation of the aorta. Circulation. 1988;78:142–8.

20. Bradley WG. Flow phenomena in MR imaging. AJR Am J Roentgenol. 1988;150:983–94.

21. Edelmann RR. Basic principles of magnetic resonance angiography. Cardiovasc Intervent Radiol. 1992;15:3.

22. Kastler B, Patay Z, Vetter D. Imagerie du flux. in Comprendre l'IRM. Paris: Masson; 2006 (6th edition). P. 189–214.

23. Kastler B. Principles of MR angiography. In: Patay Z, Kastler B, Anzalone N, editors. Applied neuroMR angiography CD-ROM. Antwerpen: Lasion; 1996.

24. Holmqvist C, Larsson EM, Stahlberg F, Laurin S. Contrast-enhanced thoracic 3D-MR angiography in infants and children. Acta Radiol. 2001;42:50–8.

25. Lohan DG, Krishnam M, Saleh R, Tomasian A, Finn JP. MR imaging of the thoracic Aorta. Magn Reson Imaging Clin N Am. 2008;16(2):213–34.

26. Lohan DG, Krishnam M, Saleh R, Tomasian A, Finn JP. Time- resolved MR angiography of the thorax. Magn Reson Imaging Clin N Am. 2008;16(2):235–48.

MRI with its large field of view, excellent spontaneous vessel-tissue contrast, good spatial resolution, and functional approach to blood flow is very well adapted to visualization of cardiac as well as mediastinal structures, in contrast with echocardiography, which is limited by bone or air artifacts [1–15]. However, as for any "tomographic" technique, multiplanar MRI requires mental 3D reconstruction of cardiovascular anatomy from a series of sequential images 3–10 mm thick, obtained after processing.[1]

A good knowledge of normal cardiac anatomy in the "useful" imaging planes usually performed (axial, coronal, sagittal, and guided according to the anatomical axis of the heart) is therefore an essential prerequisite. This approach allows segmental cardiovascular analysis[2] [16–20] by identifying the various cardiac chambers and great vessels, their location, and their mode of connection.

Healthy subjects with usual connections (SVC and IVC → RA → RV → PA and PV → LA → LV → Ao[3]) present a right–left arrangement of cardiac chambers which is correlated with the thoracic and abdominal arrangement. Due to the orientation of the anatomical axis of the heart, the "right" chambers are actually in a "right anterior" position compared to the "left" chambers, which are situated in a "left posterior" position (Figs. 2.1–2.3). Furthermore, due to crossover (twisting) of the great vessels at their origin, the pulmonary artery and aorta do not comply with this right–left symmetry. At its origin, the ascending aorta ("left-sided" structure) is situated centrally and posteriorly (and to the right) of the pulmonary artery ("right-sided" structure), which is situated anteriorly (and to the left) (Figs. 2.1 and 2.4).

Many variants of position and cardiac and vascular connection (inversion) can be observed in congenital malformations. The various chambers (atria/ventricles) are therefore identified by morphological criteria as "morphologically right" (mRA, mRV) or "morphologically left" (mLA, mLV) regardless of their actual position ("right" or "left").

After a general review of the principles of cardiovascular imaging and a few basic concepts, this chapter describes cardiovascular anatomy, illustrated by an atlas of normal imaging, which is completed by segmental sequential analysis (see Chap. 3).

## 2.1 General Principles

MRI examination, particularly in children, requires perfect sedation (or possibly even general anesthesia), as the slightest movement can significantly alter the image quality (see Chap. 1).

After a localizing sequence, the examination starts with axial spin-echo sequences, providing a precise and reliable three dimensional tomographic visualization of cardiovascular anatomy. On T1-weighted spin-echo-based sequences, the blood, circulating rapidly in vessels and cardiac chambers, usually generates spontaneous contrast ("low signal intensity" – black) compared to mediastinal fat ("high signal intensity" – white) and soft tissues (vessel walls and myocardium, "isosignal" – gray). Chambers and airways (lungs, trachea, etc.),

---

[1]Real-time imaging is possible on more recent machines, which allows selection, on a beating heart image, of the most appropriate imaging plane to visualize the structure of interest.
[2]In the same way as for echocardiography, angiography or autopsy.
[3]SVC and IVC = superior vena cava and inferior vena cava, RA and LA = right and left atrium, RV and LV = right and left ventricle, PA = pulmonary artery and Ao = aorta.
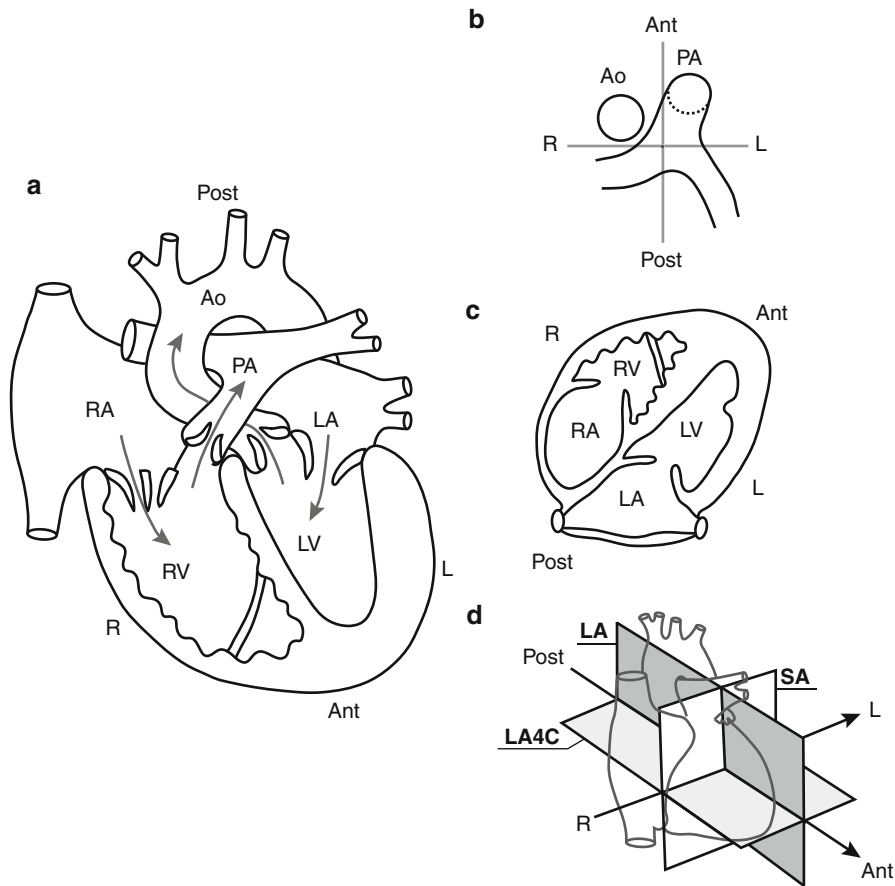
**Fig. 2.1** Normal arrangement of cardiac chambers and great vessels. (**a**) Anatomical diagram, (**b**) Section through the origin of the aorta (Ao) and pulmonary artery (PA), (**c**) "Four-chamber" axial image. (**d**) Diagram of the arrangement of the cardiac chambers in the thorax. (**a**) The aorta (Ao) emerges from the (morphologically) left ventricle (LV-mLV), and the pulmonary artery (PA) emerges from the (morphologically) right ventricle (RV-mRV). (**b**) At its origin, the ascending aorta is in a central position, posteriorly and to the right of the pulmonary artery, which is situated anteriorly and to the left. (**c**, **d**) "Right" chambers are "right anterior" and "left" chambers are "left posterior" (also see Figs. 2.2 (anatomical axis) and 2.4 (short-axis and long-axis images) and Figs. 2.4, 2.6, and 2.7 ("four-chamber" axial images). Right atrium (RA) and left atrium (LA). Note that the loop rule indicating that both the Ao and mRV are situated on the same side applies here (*see below*)

bone and calcifications also appear black (see Chap. 1). The field of view is adapted to the child's thorax including the heart, mediastinum, lungs, and extends into the neck or even the abdomen to analyze the position of abdominal viscera.

## 2.2  Choice of Imaging Planes

Although acquisition of a first series of axial images is essential, the choice of the other imaging planes (the most appropriate: other axial series, coronal, sagittal, and/or oblique series) cannot be standardized. The examination protocol is adapted to each individual case by referring to the clinical file and the problems not resolved by echocardiography, and also the information gradually obtained during acquisition of MR sequences. The use of oblique slices containing vascular structures (situated away from the heart) is sometimes very useful, as these structures are not always clearly visualized on echocardiography. The limiting factor when elaborating this examination protocol (as is often the case in imaging) is the duration of the examination. The use of rectangular fields of view with asymmetrical matrices (e.g., $96 \times 256$) and several

**Fig. 2.2** Anatomical axis of the heart. The anatomical axis of the heart or long-axis (base-apex) is usually directed anteriorly, inferiorly, and to the left. Consequently, the atria are situated posteriorly and superiorly, and the ventricles are situated anteriorly and inferiorly (see text and Figs. 2.1c and 2.5c)
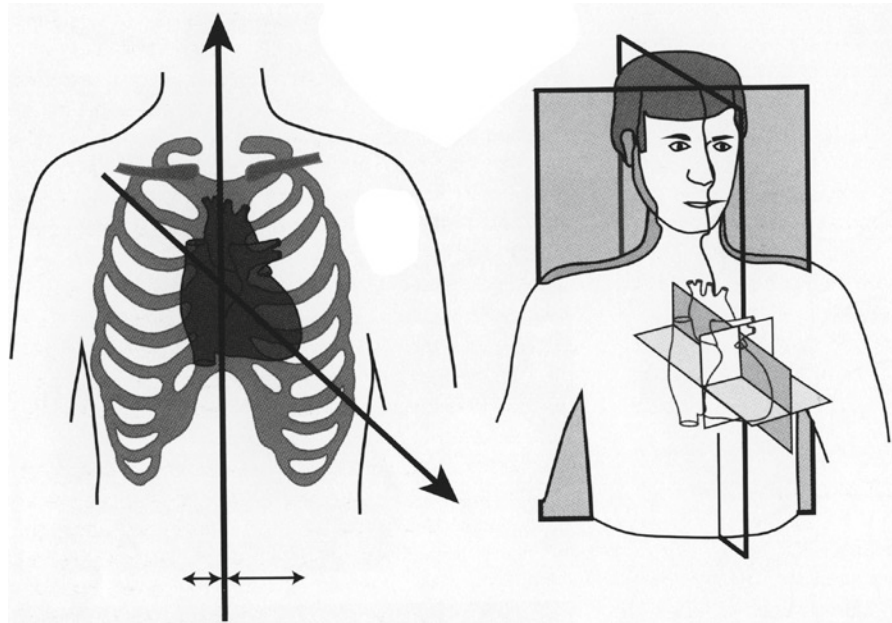
excitations (at least 4) reduces the examination time and movement artifacts [21, 22]. Under these conditions, the acquisition time of a conventional spin-echo (SE) sequence is in the range of 2–4 min (series of 5 images in a given imaging plane). Fast imaging sequences have strongly reduced imaging time down to a few seconds allowing breath-hold acquisition.4 However, the total examination time for a thorough examination comprising a series of 6–10 sequences is around 30–45 min. This procedure is well tolerated even by very young, sick, or premature patients.

To improve visualization of small vessels, we recommend two series of thin (3–5 mm), intertwined, and overlapping (2–3 mm) slices in each plane of interest.

## 2.3 Study of Blood Flow

MR study of blood flow is based on two techniques: black-blood imaging and bright-blood imaging (see Chap. 1).

### 2.3.1 Black-Blood Imaging

The spin-echo sequence (historically, the first imaging sequence to be developed) is currently the most commonly used black-blood technique for cardiac imaging. Due to long acquisition times, black blood fast spin-echo sequences have replaced traditional spin-echo sequences. In black blood fast spin-echo sequences circulating blood is generally black (as blood flows out of the slice and due to spin dephasing [23–30]). The images obtained are excellent for anatomical delineation generating "spontaneous" contrast between circulating blood which is black and soft tissues (and thrombus) which are gray (fat appears white). However, when blood circulates slowly (venous flow or end-diastole arterial flow as, for example, in aortic aneurysm or false lumen), flow effects may be confusing. An intermediate intravascular signal or even a high signal intensity due to inflowing unsaturated blood can be observed and may be mistaken for obstruction or thrombus [31]. This situation can be clarified by using sequences with saturation bands outside the Fov of interest [24, 30] (which restore the usual contrast between black circulating blood and gray thrombus) or bright-blood imaging (circulating blood is white and thrombus is gray), which is briefly discussed later [25–36].

---

4 Not always possible in practice in very young patients – feasible in elderly cooperative children and adults.
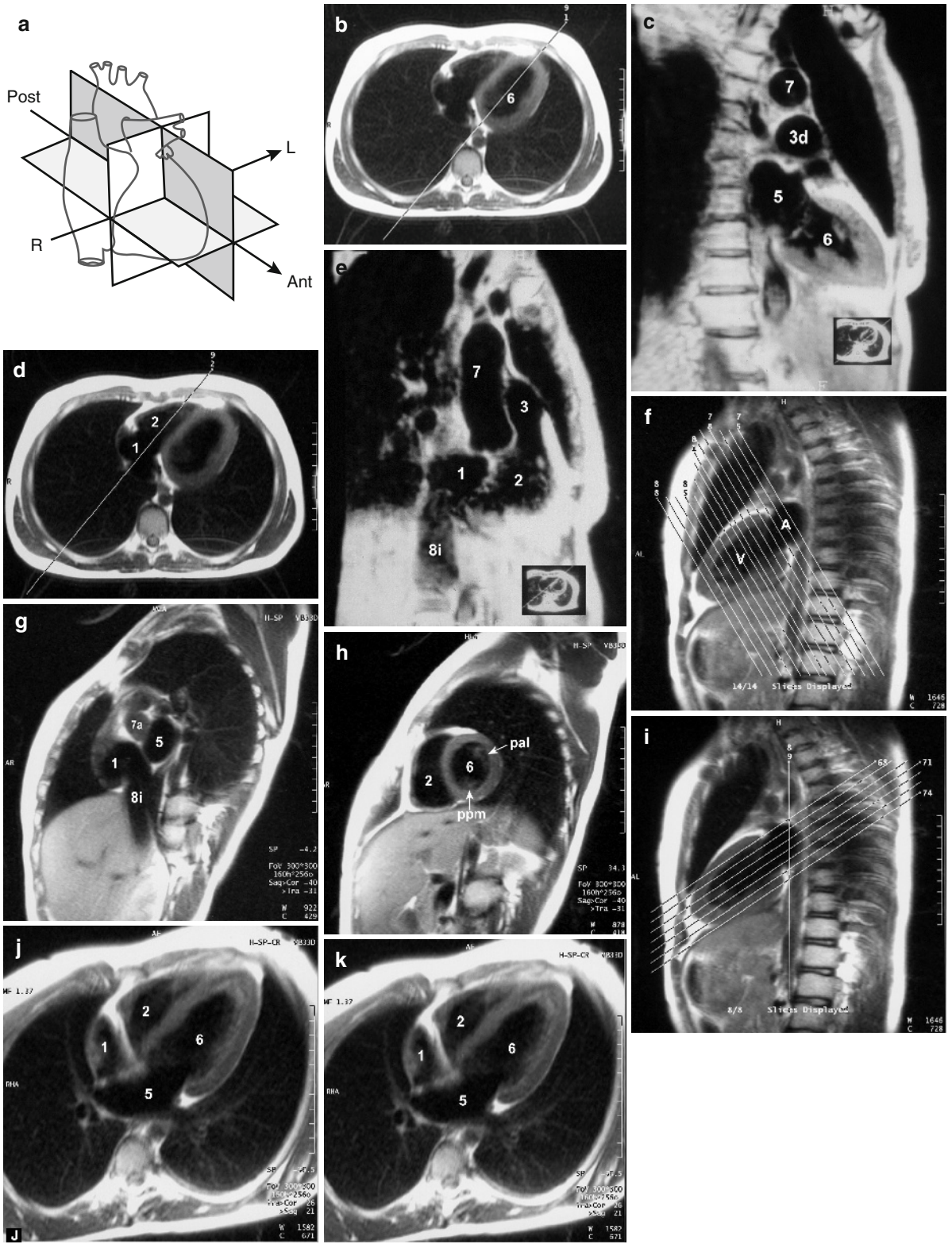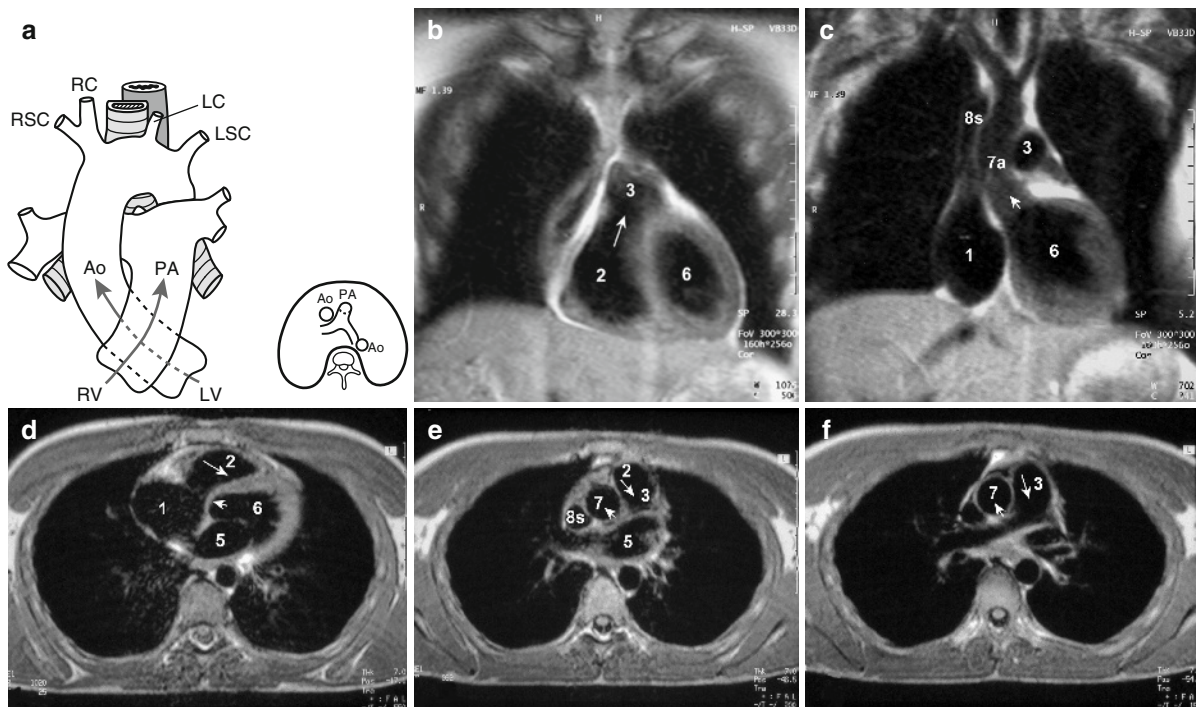
**Fig. 2.4** *Crossover* (Twisting) of the aorta (Ao) and pulmonary artery trunk (PA) at their origin. Schematic diagram (**a**) and coronal *fast spin-echo* images through the origin of the pulmonary artery (*long arrow*, 3 – **b**) and the aorta (*short arrow*, 7 – **c**). Axial *fast spin-echo* images through the origin of the aorta (**d**) and pulmonary artery (**e**, **f**). The ascending aorta (Ao-7) at its origin is in a central position, posteriorly and to the right of the pulmonary artery (PA-3) which is situated anteriorly and to the left. The vessels cross over at their origin (*short* and *long arrows*): the *pulmonary artery* emerges from the right ventricle (*2*) and the *aorta* emerges from the left ventricle (*6*); right atrium (*1*), superior vena cava (*8s*)

Incomplete blood signal suppression and respiratory motion artifacts are also potential limitations of fast spin-echo sequences. Respiratory motion algorithm or navigator echo techniques using diaphragmatic motion have hence been proposed. A double inversion pulse can be added at the beginning of the sequence for blood pool signal suppression and optimization of black blood imaging [37]. Single slice or better multislice double IR T2 weighted sequences allowing excellent image quality during one breath-hold[4] [38]) are now becoming the gold standard for black blood imaging and are used routinely, replacing fast spin-echo sequences. Black blood sequences should be performed before gadolinium injection as the latter impairs proper blood suppression by the IR pulse.

---

**Fig. 2.3** Images in the anatomical axis of the heart. (**a**) Schematic diagram. (**b**–**g**) Long-axis *two-chamber (vertical dark gray plane) and four-chamber (true four-chamber image* – horizontal light gray plane) and short-axis *two-chamber* images. The "left chamber" long-axis images (**c**) and "right chamber" long-axis images (**e**) were obtained from the axial image ("four-chamber"), by placing the imaging planes in the anatomical axis of the heart on the left (**b**) and right (**d**) chambers, respectively. Short-axis images (double oblique *true short-axis*) are obtained from the long-axis image (**f**), by placing the imaging planes perpendicular to the anatomical axis of the heart: posterior images through the atria (**g**) and anterior images through the ventricles (**h**). (**j**, **k**) Four-chamber axial images in the anatomical axis of the heart (*true four-chamber image*), obtained from the long-axis image (**f**) by placing imaging planes parallel to the anatomical axis of the heart; right atrium (*1*), right ventricle (*2*), left atrium (*5*), left ventricle (*6*), ascending aorta (*7*), inferior vena cava (*8i*), anterolateral papillary muscles (pal), and posteromedian papillary muscles (ppm)
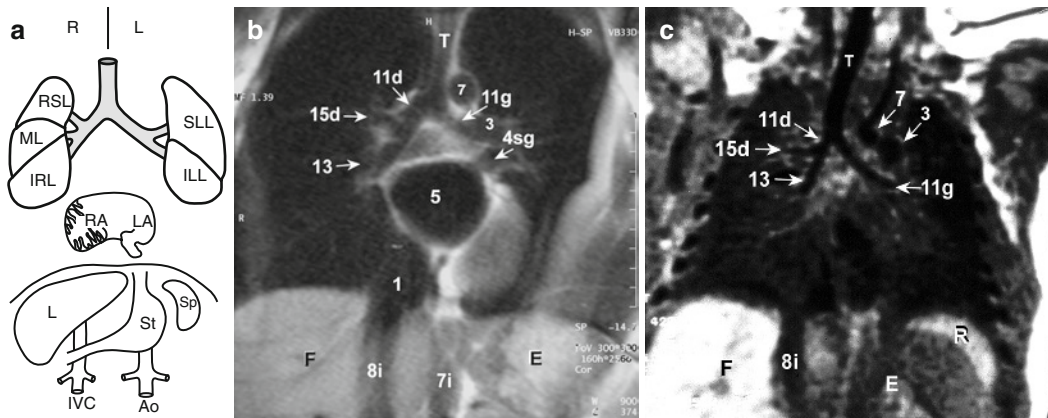
**Fig. 2.5** Correlation between the atrial, thoracic, and abdominal arrangements in situs solitus (normal atrial position). (**a**) Schematic diagram. (**b**, **c**) Coronal spin-echo images in a child (**b**) and an infant (**c**). Right-left pulmonary asymmetry: right main bronchus (11d) on the right and left main bronchus (11g) on the left correlated with the atrial positions; right atrium (RA-1) on the right and left atrium on the left (LA-5). The same applies to the position of abdominal organs: Liver (L) on the right and spleen (Sp) and stomach (St) on the left, inferior vena cava (IVC-8i) on the right and abdominal aorta (Ao-7i) on the left. Right upper lobe (RUL), left upper lobe (LUL), middle lobe (ML), right lower lobe (RLL), left lower lobe (LLL); pulmonary artery (left-3), left superior pulmonary vein (*4sg*), ascending aorta (*7a*), left main bronchus (*11g*), *bronchus intermedius* (*13*), right upper lobe bronchus (*15d*) (also see Chap. 3, Figs 3.2 and 3.19b and Chap. 5, Fig. 5.23)

**Fig. 2.6** "Morphologically" right atrium (mRA) and "morphologically" left atrium (mLA). (**a**) Schematic diagram. (**b**) Axial images in an infant. (**c**, **d**) Axial images in a young adult. The "morphologically" right atrial appendage (*1d*) has a triangular shape with a broad implantation on the right atrium (*1*) (situated on the right) which is connected to the superior vena cava (*1*). The "morphologically" left atrial appendage (*5g*) has a finger-like shape with a narrow implantation on the left atrium (*5*) (situated on the left); pulmonary infundibulum (*2i*) below the pulmonary artery, right superior (*4sd*), right inferior (*4id*), and left inferior (*4ig*) pulmonary veins, ascending and descending aorta (*7 and 7d*), superior vena cava (*8s*); note the origin of the right coronary artery (*20*) (also see Chap. 3, Fig. 3.19b)
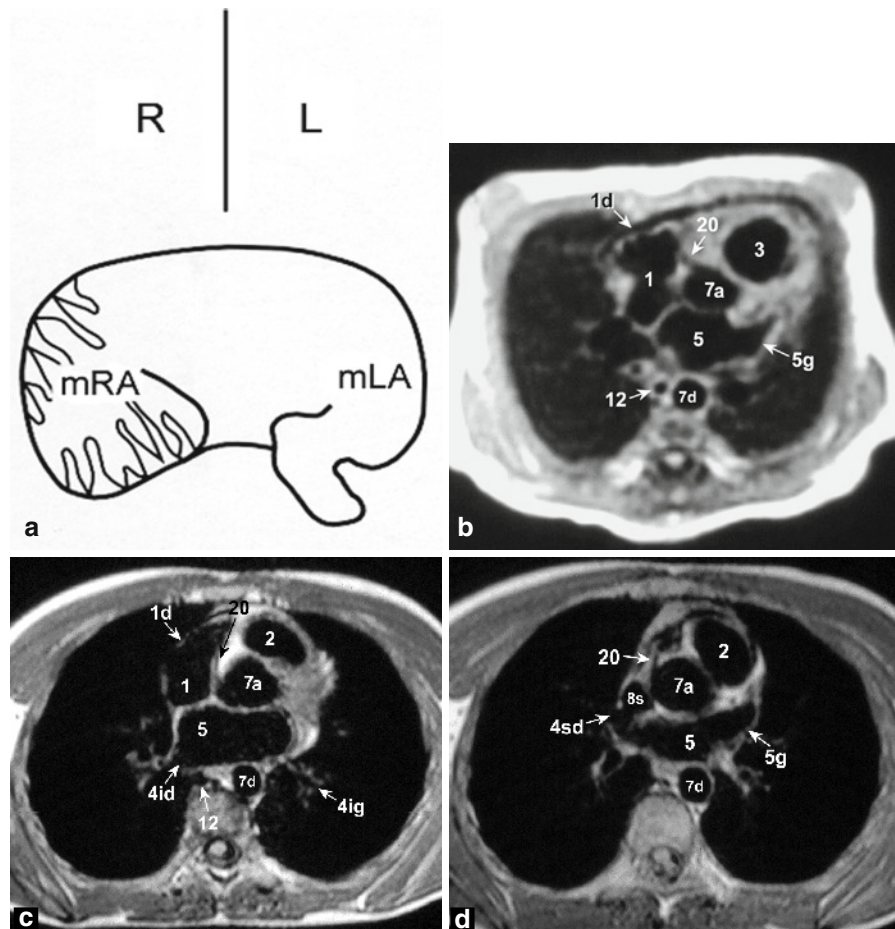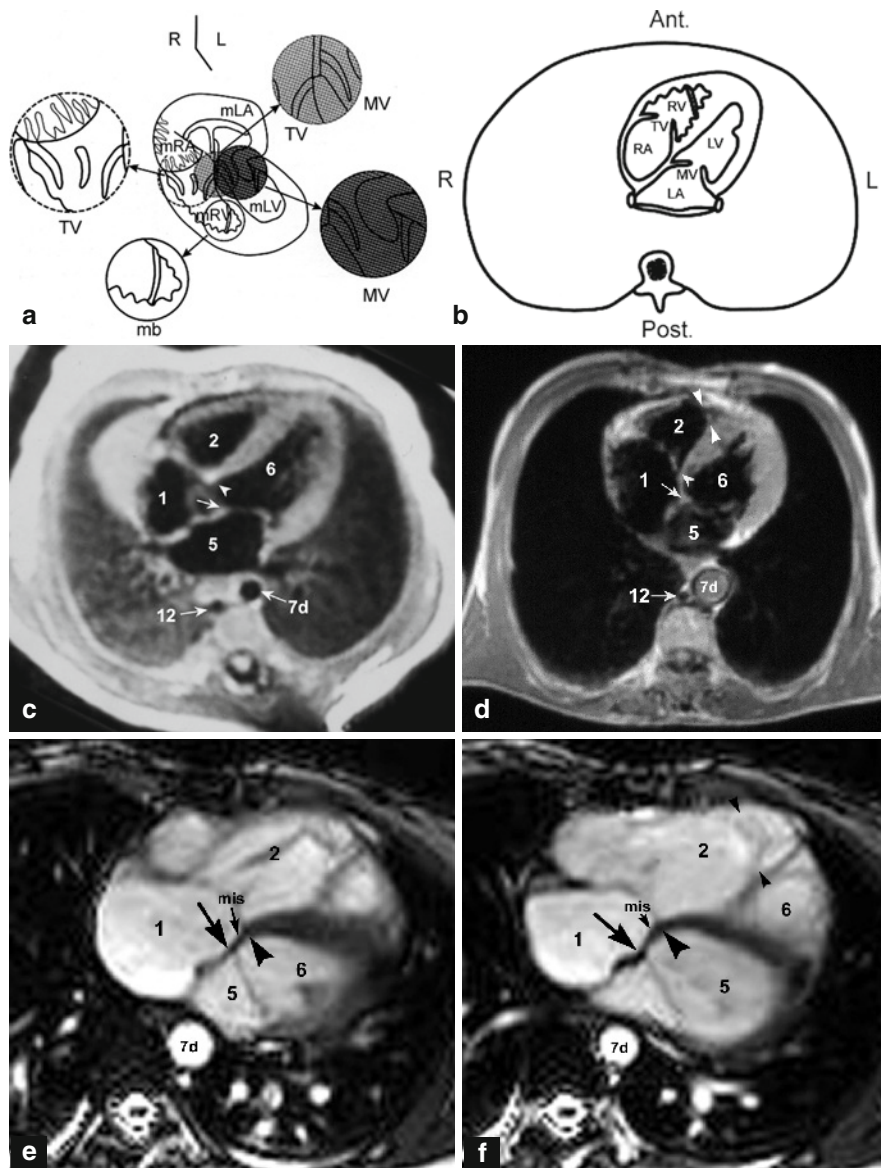
**Fig. 2.7** "Morphologically" right ventricle (mRV) and "morphologically" left ventricle (mLV). (**a**) Schematic diagram. (**b**) "Four-chamber" axial spin-echo images through the ventricular chambers in an (**c**) and an adolescent (**d**). Gradient-echo cine-MR axial images (**e** and **f**). Morphologically right atrium (mRA) and left atrium (mLA). Identification of mRV and mLV is based on the insertion of the atrioventricular valve leaflets in relation to the interventricular septum: the tricuspid valve (TV– *arrowhead* - not VM) which always opens into an mRV, is always situated more anteriorly (and inferiorly to the apex of the heart) compared to the mitral valve (MV– *arrow*), which always opens into an mLV and which is situated more posteriorly. This offset of the valves delineates the membranous interventricular septum (mis). The mRV is also identified (second criterion) by the presence of trabeculations and the moderator band (between *arrow heads*); right atrium (*1*) and left atrium (*5*), right ventricle (*2*) and left ventricle (*6*), descending aorta (*7d*), azygos vein (*12*) (also see Chap. 3, Figs. 3.17c and d, 3.19c, 3.20e, 3.21b, and 3.24d and Chap. 7, Fig. 7.14 and Chap. 8, Figs. 8.14 and 8.22)

## 2.3.2 Bright-Bood Imaging

Bright-blood imaging techniques give physiologic information on blood flow. Bright-blood imaging uses gradient-echo (GE) sequences with flow compensation (circulating flow-white and soft tissues-dark gray). The acquisition time is sufficiently short to allow breath-hold images[4] [25–27]. They provide dynamic ECG-gated cine-MRI images [25–27, 33–36, 39, 40], or MR angiography images [28–31] on which soft tissues are